NASA CONTRACTOR REPORT

NASA CR-1336

EFFECT OF FREE STREAM TURBULENCE ON COAXIAL MIXING

by R. A. Kulik, J. J. Leithem, and H. Weinstein

Prepared by
ILLINOIS INSTITUTE OF TECHNOLOGY
Chicago, Ill.
for Lewis Research Center

NATIONAL AERONAUTICS AND SPACE ADMINISTRATION • WASHINGTON, D. C. • MAY 1969

NASA CR-1336

EFFECT OF FREE STREAM TURBULENCE ON COAXIAL MIXING

By R. A. Kulik, J. J. Leithem, and H. Weinstein

Prepared under Grant No. NsG-694SC by
ILLINOIS INSTITUTE OF TECHNOLOGY
Chicago, Ill.

for Lewis Research Center

NATIONAL AERONAUTICS AND SPACE ADMINISTRATION

For sale by the Clearinghouse for Federal Scientific and Technical Information
Springfield, Virginia 22151 – CFSTI price $3.00

ABSTRACT

The effects of free stream trubulence and boundary layer trip devices on mixing in a co-axial jet stream are presented.

A screen of fine mesh placed in the outer "infinite" free stream effected both a boundary layer separation where screen and inner duct met, and a lowering of the free stream turbulence level. To determine the dominate effect of the screen, a boundary layer trip device was used to effect the boundary layer separation without reducing the free stream trubulence.

Both air-air and air-Freon-12 systems with density ratios of 1 and 4 respectively, were studied. The outer stream velocity was kept constant at 51 ft/sec and the mass average velocity ratios varied from 2 to 20.

Data is presented for the relative axial turbulence intensities as well as velocity, concentration, and mass holdup.

Comparison of the screen and boundary layer trip device data taken without any such devices indicated that both devices effected the same preservation of the inner-stream integrity. Mixing is retarded by a factor of 2 to 4 for low velocity ratios.

FOREWORD

Research related to advanced nuclear rocket propulsion is described herein. This work was performed under NASA Grant NsG-694 with Mr. Maynard F. Taylor, Nuclear Systems Division, NASA Lewis Research Center as Technical Manager.

TABLE OF CONTENTS

NOMENCLATURE

A	Intercept term for linear hot film relationship.
B	Slope term for linear hot film relationship.
C_M	Mean concentration.
C_p	Heat capacity of the gas.
D	Diameter of the hot film.
k	Thermal conductivity of the gas.
K_f	Emperical coefficient in Kramer's equation.
K_g	Emperical coefficient in King's equation.
L	Length of the hot film.
P	Power dissapation from the hot film.
P_e	Pressure.
R	Gas constant.
r_o	Radius of inner stream orifice.
t	Time.
T_g	Temperature of the gas.
T_o	Time interval for time averaging process.
T_w	Temperature of the hot film.
U	Axial velocity component.
U_e	Effective cooling velocity for the hot film.
u	Fluctuating axial velocity component.
V	Radial velocity component.
v	Fluctuating radial velocity component.
x	Distance.

ϵ Eddy kinematic viscosity.

β Temperature coefficient of a thermistor.

ρ Density.

η Molecular viscosity

INTRODUCTION

Turbulent mixing of coaxial jets finds many physical applications. Among these applications are thrust augmentation devices, jet engine afterburners, jet engine combustion chambers, ejectors and the gaseous core nuclear rocket.

Coaxial jets have been investigated since 1925. Initial investigations were concerned mainly with laminar jets. Later investigations delt mainly with homogeneous turbulent flows.

The extension to heterogeneous flow systems has been a recent development coming with the advent of jet and rocket propulsion systems.

It is the object of this work to present velocity and turbulence quantities in a homogeneous flow system both close and far downstream, and velocity, density, turbulence and mass holdup quantities in a heterogeneous flow system both close and far downstream. The density ratio for the heterogeneous case treated was 4 to 1, inner to outer stream. The outer stream turbulence level was brought below its free stream value by a screen placed in the outer stream just upstream of the mixing region. The screen affected both the turbulence intensity of the outer stream and because of its proximity to the jet orifice, the boundary layer that developed on the outside of the injection tube. An attempt to separate these two effects was made using a boundary layer trip device on the outside of the injection tube, affecting only the boundary layer.

BACKGROUND

Boussinesq[1], Prandtl[2], Taylor[3], Von Karman[4], and Reichardt[5] all advanced theories on turbulent mixing. Of the various theories, Prandtl's and Taylor's are still used because of their simplicity and Reichardt's is used because of its close agreement with experimental results.

Coaxial flow systems were investigated by Tani and Kobashi[6,7], Boehman[8], Alpinieri[9], Zawacki[10], D'Souza[11], and Montealegre[12]. Tani and Kobashi reported the axial and radial turbulence intensities and the turbulent Reynold's stress for a homogeneous system. Forstall and Shapiro[13] reported velocity and density profiles where helium tracer was used in the inner stream. This still resulted in a density ratio very close to 1. Boehman[8] also used a tracer in the inner jet to avoid density gradients. He developed an expression for the radial eddy kinematic viscosity, ϵ, which was nearly constant over the mixing region and decreased to zero at the edge of the mixing region. Alpineri[9] reported on a heterogeneous coaxial system. He considered the equal mass flow rate and equal velocity cases. He found that ϵ varied with axial position. Zawacki reported turbulence quantities both near and far downstream for a coaxial flow system with density ratios of 1, 4 and 7, with velocity ratios ranging from 1 to 30. D'Souza and Montealegre both reported data on coaxial jet mixing for a heterogeneous system with a density ratio of 4 at various velocity ratios.

Frenkeil, Howard and Laurence, and Conger have reported the effect of grids on the turbulence downstream of the grid. Frenkiel[14] found that for large Reynolds numbers of turbulence, the data agreed well with theory. Howard and Laurence[15] found that the grid redistributes the turbulent energy spectrum from a low to a high frequency range. They also reported that the scale of turbulence is a linear function of distance from the grid and is greater than for a similar flow system without a grid. Conger[16] measured velocity, concentration and turbulence quantities downstream of a grid. The system was such that the velocity and concentration fluctuations were linearly independent. This is not true however for the coaxial jet system where density and velocity gradients are superimposed.

Recently, Johnson and Clark[17] investigated the heterogeneous mixing region in the near downstream region in a double coaxial jet. They found that the inner stream integrity could be maintained further downstream with the double coaxial jet than in the single coaxial jet. They, as did Zawacki, noted the presence of recirculation cells at the mouth of the jet.

HOT WIRE ANEMOMETRY

The hot wire anemometer is the most sensitive and accurate instrument presently available for the study of turbulent flow. The frequency response of a hot wire anemometer is fast enough to permit measurement of the turbulent properties of the flow system. There are two types of anemometer in use today, the constant current and the constant temperature. The sensing element for either system is basically the same, a small wire or themistor with a high resistivity or β factor respectively. The higher the resistivity or β factor, the greater will be the probe's change in impedence for a given change in temperature.

The constant current hot wire anemometer system supplies a constant current to the probe and the unbalance caused in a Wheatstone or Kelvin Bridge is used as a measure of the heat transferred from the probe to the fluid.

The constant temperature hot wire anemometer system maintains the balance of the bridge circuit and uses the power needed to maintain the balance as a measure of the heat transferred.

The heat transferred from a probe to the surrounding fluid is a function of the velocity of the fluid past the probe, the temperature difference between the fluid and the probe, the physical properties of the fluid and the dimensions and physical properties of the probe.

The problem of heat transfer from small heated cylinders was solved by King[18]. King gave the following relationship:

$$P = K_g L (T_w - T_g) \left[1 + \left(\frac{2\pi\rho_g C_p DU}{K_g} \right)^{1/2} \right] \qquad (1)$$

for $\frac{\rho C_p DU}{K_g} > 0.08$. This gave a linear relationship between the heat lost

and the square root of velocity.

Kramer[19] also derived a linear relationship between the heat lost and square root of velocity

$$P = A + B U^{1/2} \tag{2}$$

$$A = L \pi K_f (T_w - T_g)(0.42)\left(\frac{C_p \eta}{k}\right)^{1/5} \tag{3}$$

$$B = L \pi K_f (T_w - T_g)(0.57)\left(\frac{C_p \eta}{K_o}\right)_f^{1/3} \left(\frac{\rho D}{\eta}\right)_f^{1/2} \tag{4}$$

which he derived by substitution of an emperical equation of heat transfer into the equation of heat transfer from a cylinder.

In practice neither King's nor Kramer's equations are used, rather A and B are determined experimentally while the form of the equation is assumed to hold.

For homogeneous flow systems the average power lost by a probe can be shown to be given by:

$$\bar{P} = A + B \bar{U}^{1/2} \tag{5}$$

and the fluctuating power lost by a probe can be given by

$$P' = B \bar{U}^{1/2} \frac{u'}{2 \bar{U}} \tag{6}$$

Combining Equations 5 and 6 yields:

$$2 \frac{\sqrt{\overline{P'^2}}}{P - A} = \frac{\sqrt{\overline{u'^2}}}{\bar{U}} \tag{7}$$

where $\frac{\sqrt{\overline{u'^2}}}{\bar{U}}$ is defined as the axial turbulence intensity for a homogeneous system.

For the heterogeneous system, Equation 5 still holds for the average power lost. The fluctuating power however is more complicated and is given by Equation 8.

$$\overline{P'^2} = \left(\frac{\partial P}{\partial \rho}\right)_U^2 \overline{\rho'^2} + 2 \left(\frac{\partial P}{\partial \rho} \frac{\partial P}{\partial U}\right) \overline{\rho' U'} + \left(\frac{\partial P}{\partial U}\right)^2 \overline{u'^2} \qquad (8)$$

Using two probes of differing diameters allows Equation 8 to be applied twice to form two independent equations in three unknowns.

Both the average and the lower limit of the fluctuating density can be measured with an aspirating probe. The aspirating probe consists of a hot film probe placed in front of a sonic nozzle. Since the average sonic velocity is strictly a function of concentration in the system under consideration, the average velocity measured by the probe is a measure of only the average concentration of the gases.

The fluctuating density, as given by the RMS power disipation of the aspirating probe can be assumed to be damped because of shear mixing in the throat of the sonic nozzle.

It has been shown by Montealegre[12] that the value of ρ'^2 is so small that the error involved in solving for the other two variables $\rho' u'$ and u'^2 masks the effect of a change in ρ'^2. For an initial value of ρ'^2 Montealegre used the following relationship:

$$\rho'^2 = \frac{P'^2}{\left(\frac{\partial P}{\partial \rho}\right)^2} \qquad (9)$$

and this value of ρ'^2 was found to be sufficiently accurate to be used in Equation 8 to obtain an initial u'^2. He further showed that reasonable values of ρ'^2 can be

assumed and thus limit the range of $\rho' u'$ and u'^2 giving a reasonable estimate for u'^2.

A complete derivation of the equations and a more complete presentation of the relationships mentioned are given in a paper by Zawacki[10] and in the authors'[20,21] earlier publications.

EXPERIMENTAL INVESTIGATION

Figure 1 illustrates the apparatus used in this investigation. The main test column had an 8" square cross section and was made of 3/4" plexiglass. A Buffalo Forge type 6E, low pressure drop, high capacity blower was used to pull room air down the column. The flow rate of air in the outer stream was controlled by a large butterfly valve in the duct to the blower.

The inner stream of air or Freon-12 was introduced into the test column by a drawn stainless steel tube with a 3/4" outer diameter and a 0.0135" wall thickness. The tube was of sufficient length to assure fully developed turbulent flow. The tube was purposely chosen small compared to the test section so that the assumption of negligible outer stream wall effects could be made. Data was taken first with a 64 mesh screen placed 5 1/2" above the jet outlet. Next data was taken with a boundary layer trip device positioned 5 1/2" above the jet outlet. Figures 2 and 3 show the screen and boundary layer trip device respectively.

The 64 mesh screen was held tight by sandwiching the outer perimeter in the seam between the 24" entrance region and the 36" test section and gluing the screen to the outer wall of the injection tube with silicone rubber. The boundary layer trip device consisted of a 3/4" O-ring 1/16" thick slipped over the injection tube.

A traversing mechanism designed by L. Boehman that permitted both axial and lateral positioning of the probes was used. A 4" port was cut in the test section to permit easy changing of the probes. This port was sealed flush with the inner wall of the test section while the data was being taken. The outer wall boundary layer and the corner circulation patterns were not of sufficient magnitude to affect the jet mixing.

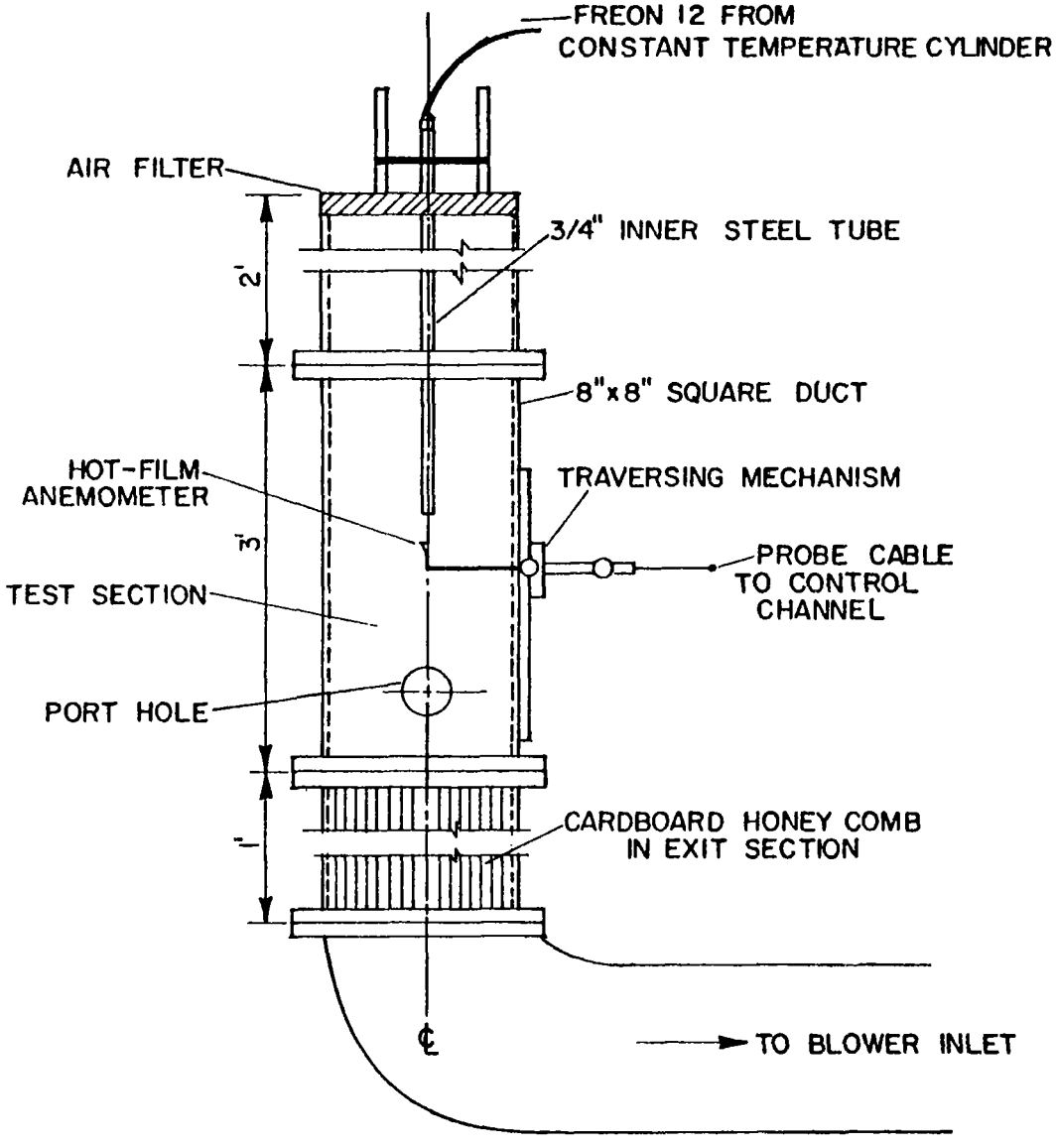

TEST SECTION

FIGURE 1

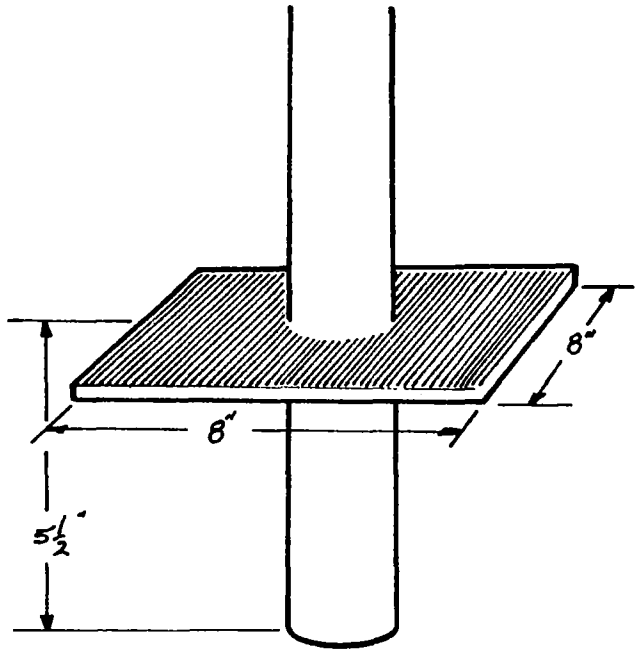

FIGURE 2 SCREEN POSITION

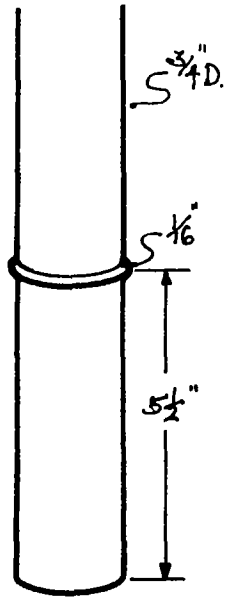

FIGURE 3 BOUNDARY LAYER TRIP DEVICE

Three high precision Brooks rotameters were used to meter the air and the Freon-12 to both the calibration apparatus and the testing apparatus. The rotameters gave a continuous range of air flow from 0.1 SCFM to 50 SCFM at 65 psig. Two Acme Cash high flow pressure regulators were used in the line ahead of the rotameters to regulate the outlet pressure of the gas. Needle valves in parallel with standard gate valves were used upstream of the rotameter to closely regulate the flow.

Air for the inner stream was supplied by a small two stage compressor. A stream jacketed vessel capable of holding three cylinders, was used to heat the Freon-12 cylinders to maintain the pressure.

A Nichrome heated section of galvanized pipe just ahead of the pressure regulator was used to add further heat to the Freon-12 stream to prevent Freon condensation in the rotameters. The external air stream was room air pulled through the top of the column. An air conditioning filter was fixed in place atop the column to prevent damage to the anemometer sensors. The outer stream velocity was set with a butterfly valve, using a calibrated sensor to determine the desired position of the valve.

The entire anenometry instrumentation was supplied by Thermo Systems Incorporated. The anenometer system consisted of two independent constant temperature anemometer channels. Each channel consisted of a bridge circuit and a power consumption computer, allowing the power needed to maintain a sensor at a given temperature to be given directly in terms of voltage. A Hewlitt-Packard root mean square voltmeter was supplied to measure the true root mean square voltage of a signal, allowing turbulence quantities to be measured. A Tektronix 502A dual beam oscilloscope was used to monitor the outputs of each of the channels. A Vidar digital voltmeter was used to display the output of the constant temperature anemometer.

Three types of probes were used in this investigation:

a. A single hot film 0.002" in diameter and 0.04" in length

b. A parallel wire probe with one wire the same dimensions as that of the single hot film probe and the second a 0.0015" diameter by 0.02" long wire. The wires were closely mounted parallel to each other on the same probe holder.

c. An aspirating probe, which consisted of a 0.001" diameter hot film mounted in a 0.08" diameter tube. A jewel bearing with a 0.007-0.009" diameter hole was mounted behind the wire. Sonic velocity was achieved at the throat with a small vacuum pump.

CALIBRATION OF INSTRUMENTS

Prior to use, each probe was calibrated in a special apparatus to determine the dependence of the power output on concentration and velocity. The calibration apparatus consisted of three high precision rotameters, a fifteen foot section of 2" schedule 40 pipe and a probe holding device mounted on a plexiglass box which also served to eliminate any stray room air currents.

For six Reynolds numbers from 6,110 to 29,400 the volumetric flow rates were determined for Freon-12 concentrations of 0.0, 0.2, 0.4, 0.5, 0.6, 0.8, and 1.0. Using Zawacki's plot of $\frac{U_{ave}}{U_{max}}$ versus Reynolds number, the center line velocity was determined. The power output of the sensor was then plotted for each concentration versus $(U_{max})^{1/2}$. The slope and intercept of each of these straight line curves was then plotted against the density. This procedure was followed for both the single hot film sensors and for each of the hot films on the parallel sensor. For the aspirating probe a simpler procedure was used since velocity has no effect on the power reading. For the same concentrations of Freon-12 as were used in the hot film calibrations the power outputs of the aspirator were recorded and subsequently plotted against density.

EXPERIMENTAL PROCEDURE

For the homogeneous cases investigated, only the average and root mean square values of the power output of a single film probe were needed. The sensor was mounted in the vertical plane and was connected to a horizontal probe holder by a right angle adapter. In this manner, there was a minimum of probe holder effect on the test system. The probe was aligned under the 3/4" inner jet with a finely divided rule.

The inner stream volumetric flow rate for a particular run was set on one of the three precision rotameters. The average and root mean square values of the power were then read for various radial and axial positions.

For the heterogeneous cases investigated all three sensors were used. The average power dissipated from the single hot film was taken. Also taken were the average and root mean square power dissipation of the aspirating sensor. Finally the root mean square value of the power dissipation for each of the two parallel wires were taken. The alignment proceedure was similar to that used for the single wire. The volumetric flow rate of the Freon-12 stream was set on one of the three precision rotameters and the five sets of data were each taken at various axial and radial positions.

CALCULATION PROCEDURES

All calculations for both homogeneous and hetreogeneous cases were performed on an IBM 360-40 computer.

For the homogeneous cases, equations 5 and 7 were programmed to obtain the average velocity and turbulence intensity profiles.

For the heterogeneous cases the average power dissipation of the aspirator sensor was used to obtain the average density of the flow system. The average density could then be used to determine the slope and intercept of the single film sensor. Thus the average velocity could be determined by the square root relationship:

$$\bar{U} = \left(\frac{\bar{P} - \bar{A}(\bar{\rho})}{\bar{B}(\bar{\rho})} \right)^2 \qquad (10)$$

Equation 8, applied to each of the parallel wires and equation 9 were solved simultaneousty on the computer for the heterogeneous turbulence quantities. Since the fluctuating density given by the aspirating sensor was inherently a low value since damping occurs in the entrance region upstream of the hot film, the value of $\frac{\overline{\rho'^2}}{\bar{\rho}}$ was incremented by values of 0.1 and the other turbulence quantities calculated. Under the restraint that:

$$\left| \frac{\overline{\rho' u'}}{\sqrt{\overline{\rho'^2}}\sqrt{\overline{u'^2}}} \right| \leq 1$$

a reasonable set of turbulence quantities could be found. It has been shown by Monteleagre[22] that the size of the density fluctuations have little effect on the velocity fluctuations.

RESULTS AND DISCUSSION

Homogeneous Cases

Data taken with the 64 mesh screen in the outer stream, both near and far downstream are presented in figures 4 through 8. The general shape is very similar to that obtained by Zawacki[10]. There is some question as to whether the dip in the velocity curves is caused only by the boundary layer momentum trough as Zawacki suggested or by some other phenomenon.

The centerline velocity may in reality, especially for the near downstream cases, be opposed to that of the bulk flow. There is evidence on the basis of a mass balance taken from heterogeneous data to indicate that circulation patterns may cause material to flow upstream at the centerline, drastically changing the shape of the velocity profile. Also, a light thread when positioned along the centerline and moved towards the jet orifice was seen to change from a hanging to an upward vertical position indicating a change in the direction of flow. Since the hot wire system is unable to sense velocity direction, the data is not plotted where it was felt that the velocity was actually negative. Turbulence intensities were, however plotted as measured everywhere. Far downstream there is little question that the flow is unidirectional and the uniform acceleration of the central portion of the velocity profile with distance downstream substantiates this.

In the region just below and outside the inner tube wall there occurs a momentum trough and possible a portion of a standing back flow circulation pattern. The momentum trough is caused by the momentum defect under the inner tube wall. If only the momentum trough occurs, the entire inner stream is moving in the same direction as the bulk flow and both the inner and outer streams accelerate the momentum trough. The centerline velocity consequently must decrease since it transfers part of its momentum to the trough zone. If however, the standing circulation pattern also exists, there is a decrease in the net area for flow causing an acceleration of the fluid around the

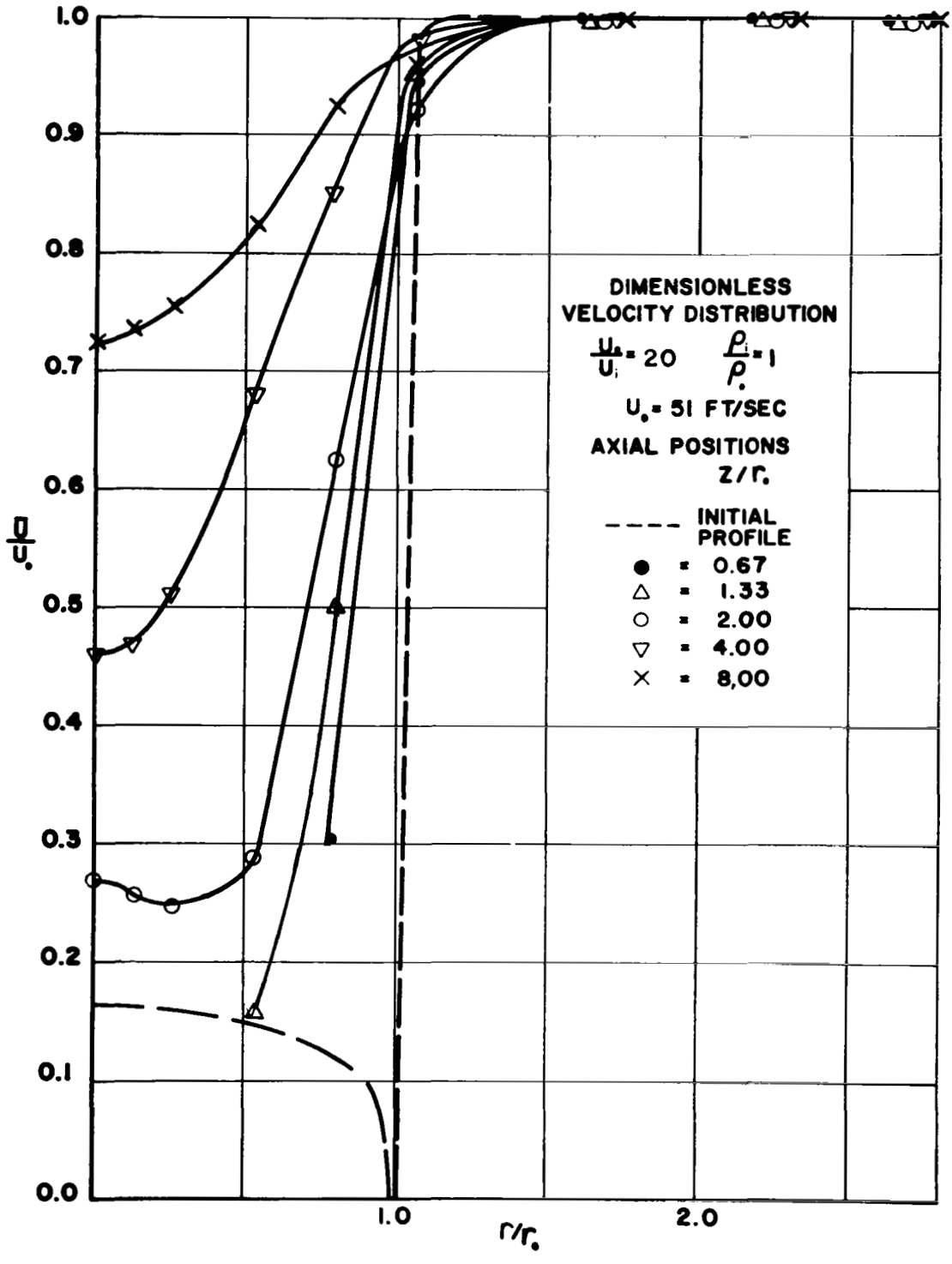

FIGURE 4

DIMENSIONLESS VELOCITY PROFILES, HOMOGENEOUS

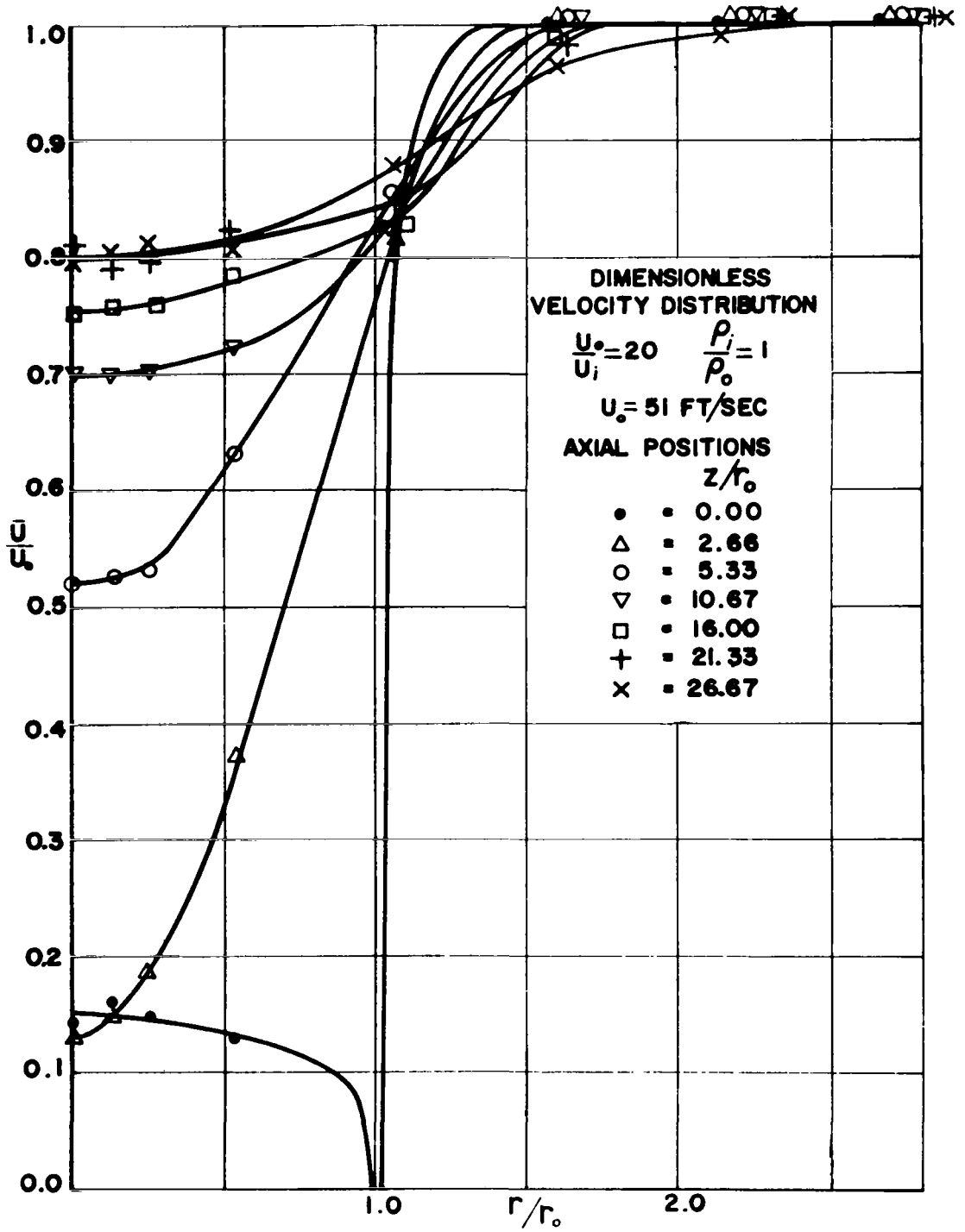

FIGURE 5

DIMENSIONLESS VELOCITY PROFILES, HOMOGENEOUS

pattern and a deceleration behind it. Momentum transfer from the outer to the inner stream in this case is greater since the center jet not only does not supply momentum to the trough zone but must be accelerated downward due to the area change. Since the centerline velocity is seen to decrease to a value lower than that observed in the trough zone, indicating momentum transfer occuring inward, it is likely that back flow does occur. Since the exact nature and extent of the back flow is not throughly known, the profiles are plotted only where the velocity was felt to be positive.
Far downstream both effects die out and the entire velocity profile is seen to be accelerated.

Figure 6 is the velocity profile along the centerline for three velocity ratios, 2, 10, and 20. In both the 20 to 1 and 10 to 1 velocity ratio cases the profiles exhibit strange behavior in the region of suspected backflow. Since the hot film sensors used were unable to make measurements in this region the profiles are shown as discontinuous. Uniform acceleration of the profiles for axial positions of $z/r_o > 4.0$, indicates unidirectional flow and so they are plotted as such.

Figures 7 and 8 show the axial turbulent intensities $\frac{\sqrt{u'^2}}{\bar{U}}$. The general behavior of the turbulence intensity profiles is to exhibit a peak which moves radially outward as axial position is increased. At an axial position of $z/r_o = 3.0$ or greater the turbulence intensity profile smooths out and decreases as expected. The curves when based on the outer stream velocity instead of the local velocity do not appear nearly so severe. They do however, retain the same general shape. This shape is caused by the initial mixing region effect noted earlier. The turbulence intensity level of the outer stream was cut about in half by the screen from the level without the screen.

Figures 9 and 10 show the velocity profiles with the boundary layer trip device substituted for the screen. The velocity profiles for the boundary layer trip device show a great similarity to those for the screen.

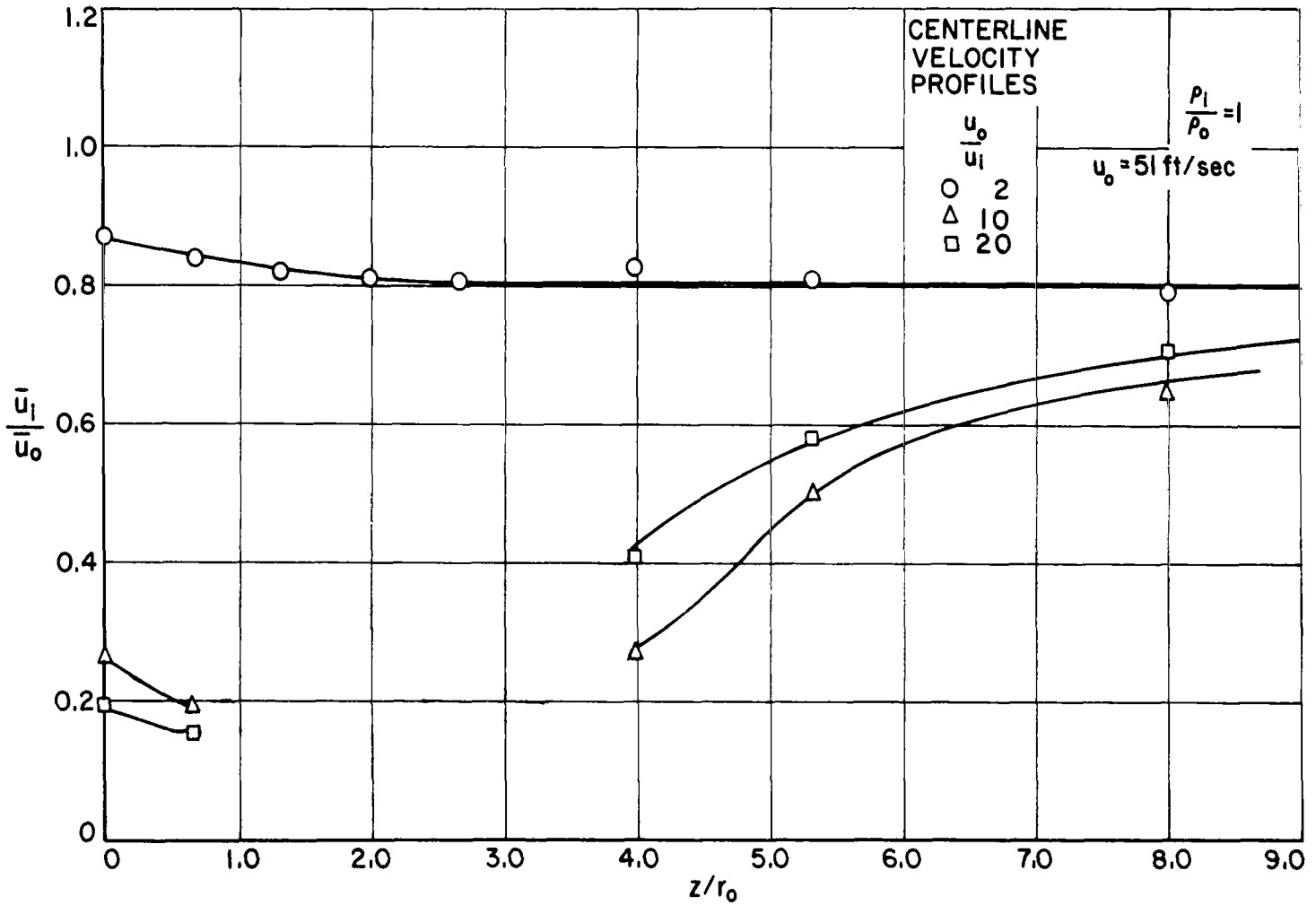

FIGURE 6

CENTERLINE VELOCITY PORFILES HOMOGENEOUS

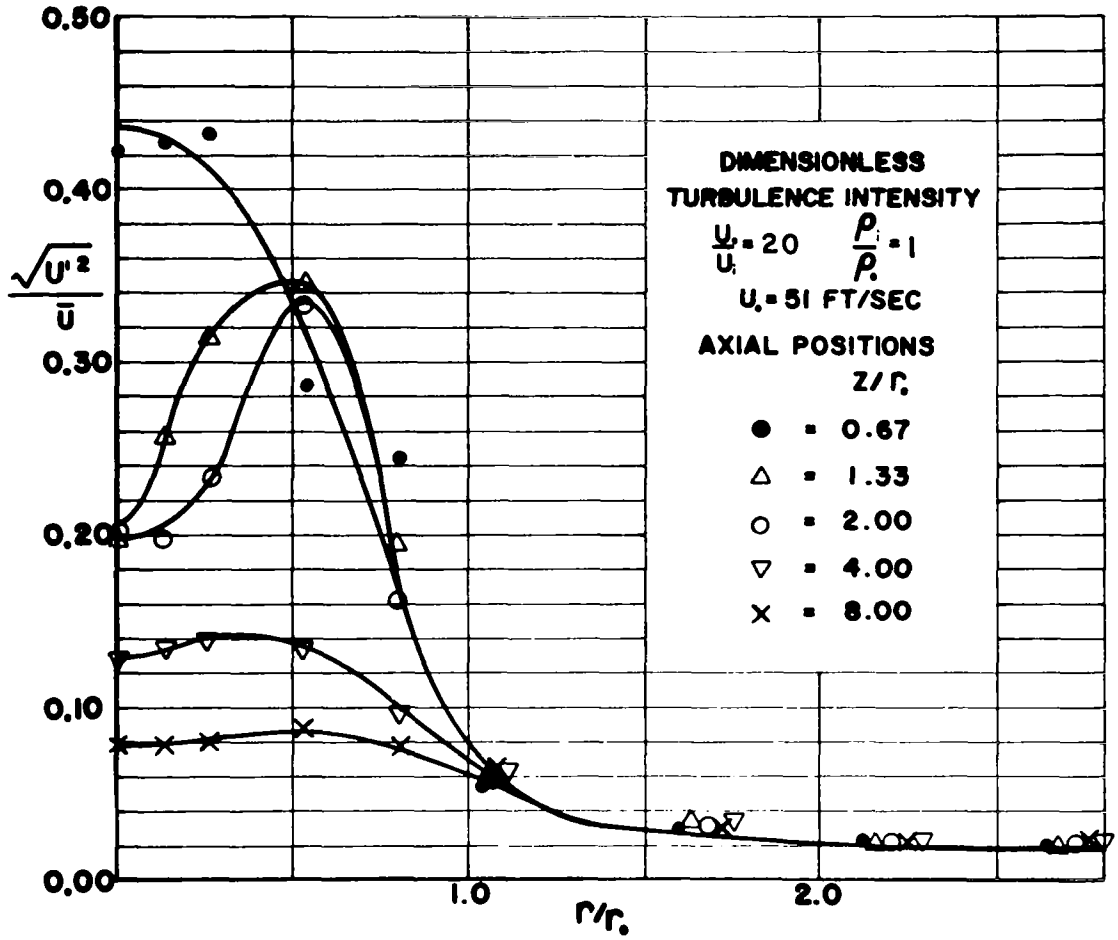

FIGURE 7

AXIAL TURBULENCE INTENSITY PROFILES, HOMOGENEOUS

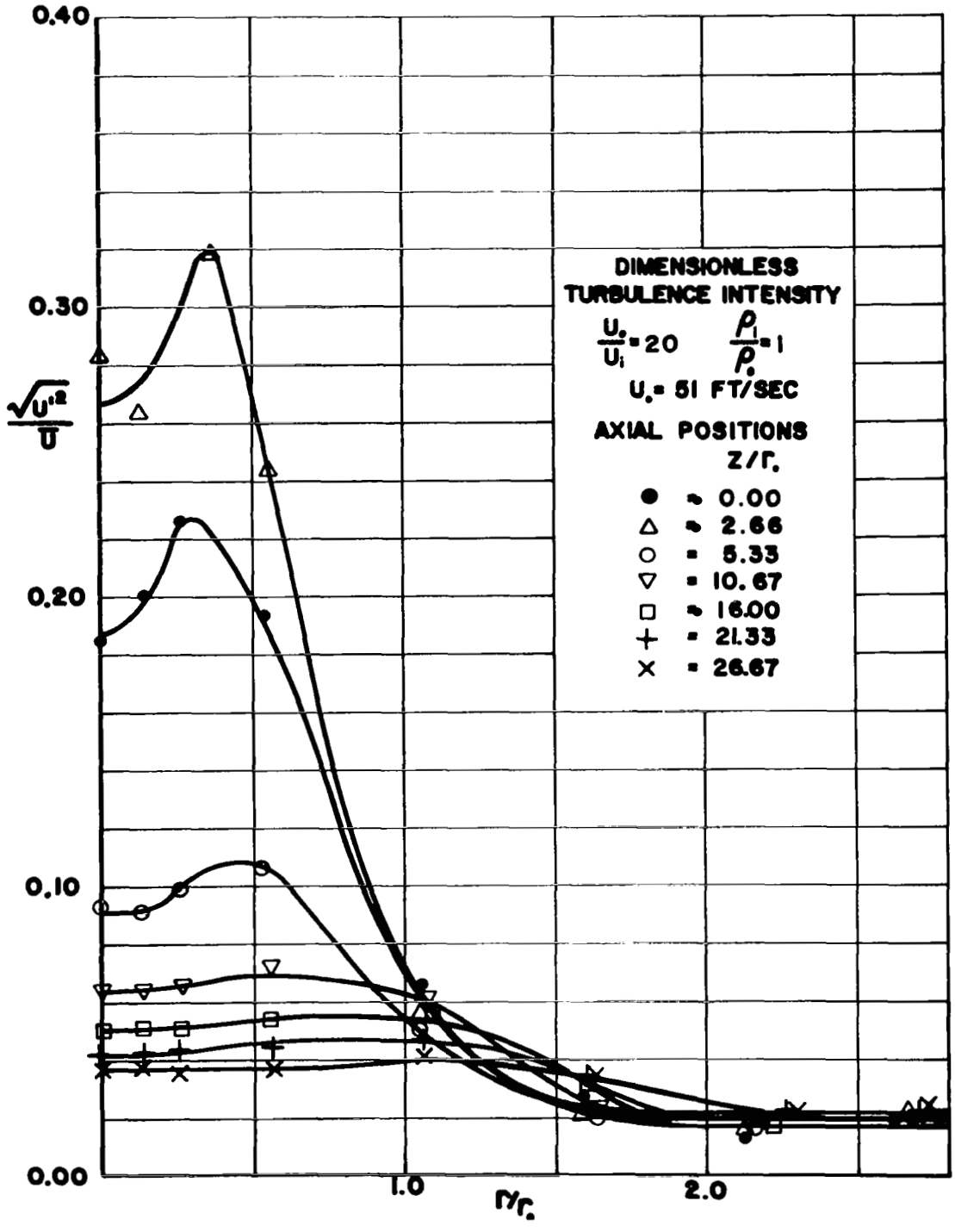

FIGURE 8

AXIAL TURBULENCE INTENSITY PROFILES, HOMOGENEOUS

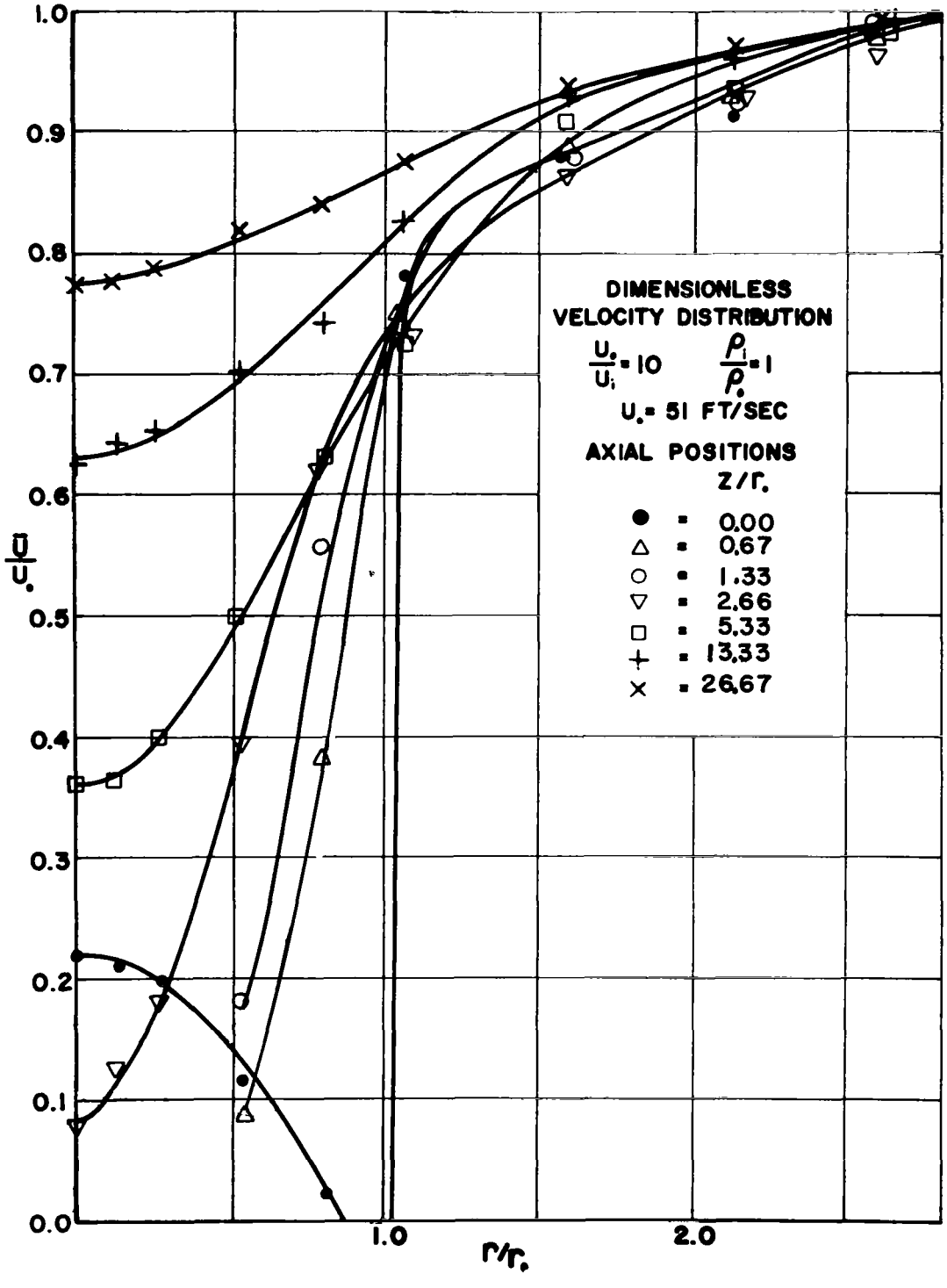

FIGURE 9

BOUNDARY LAYER TRIP DEVICE
DIMENSIONLESS VELOCITY PROFILES HOMOGENEOUS

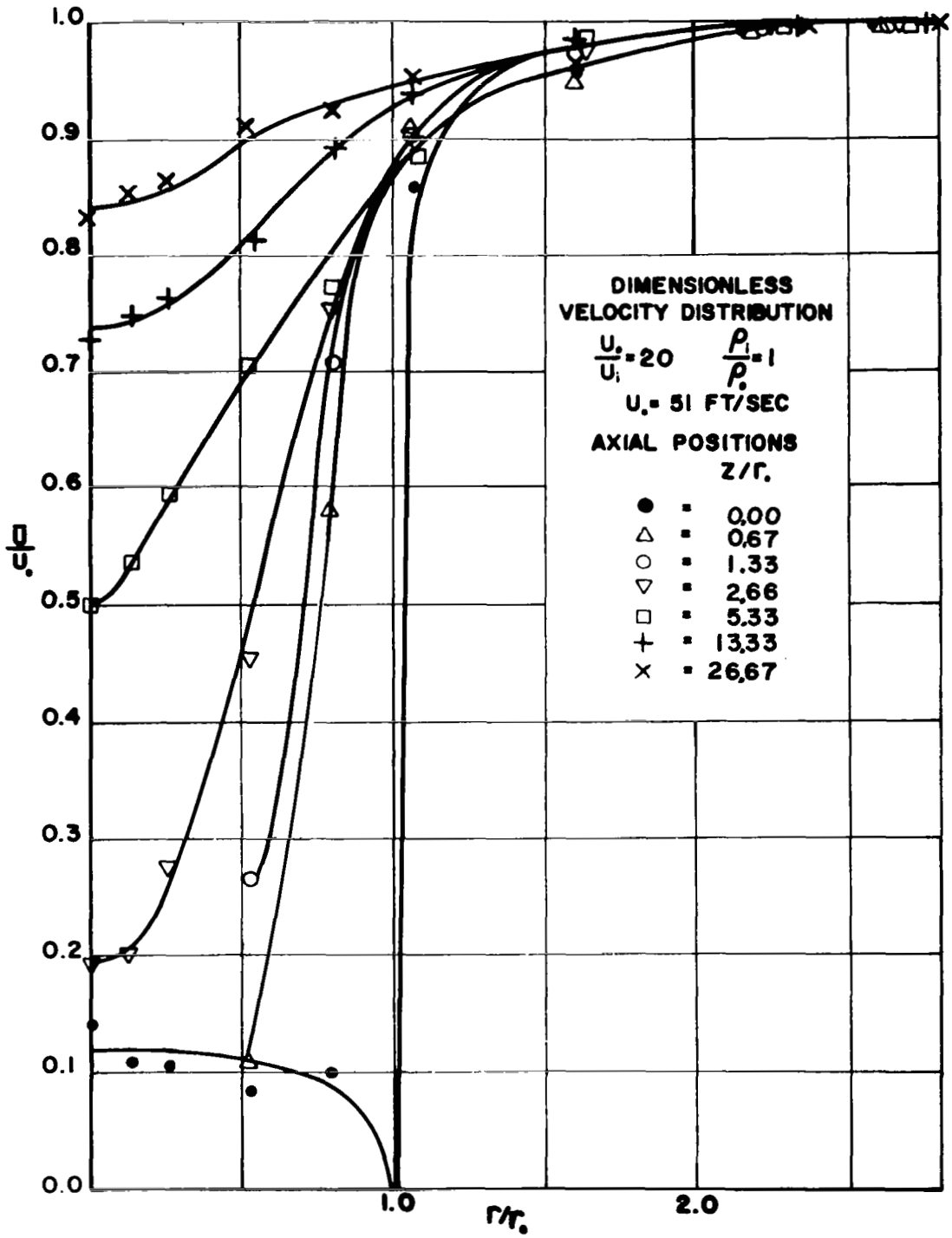

FIGURE 10

BOUNDARY LAYER TRIP DEVICE

DIMENSIONLESS VELOCITY PROFILES HOMOGENEOUS

Figures 11 and 12 show the axial turbulence intensity profiles with the boundary layer trip device in place. With the exception of the turbulence level at large values of r/r_o, the boundary layer trip device profiles exhibit the same basic shapes of those with the screen.

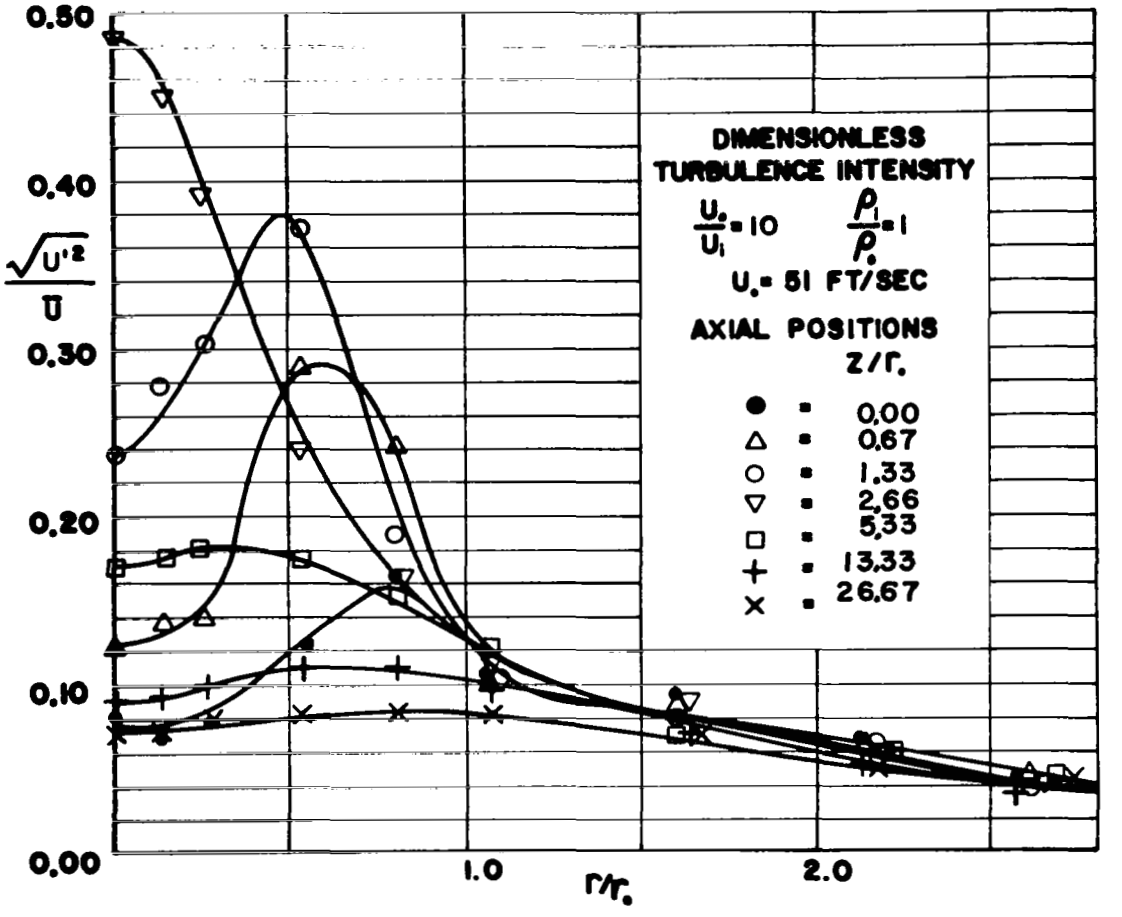

FIGURE 11

BOUNDARY LAYER TRIP DEVICE
AXIAL TURBULENCE INTENSITY PROFILES, HOMOGENEOUS

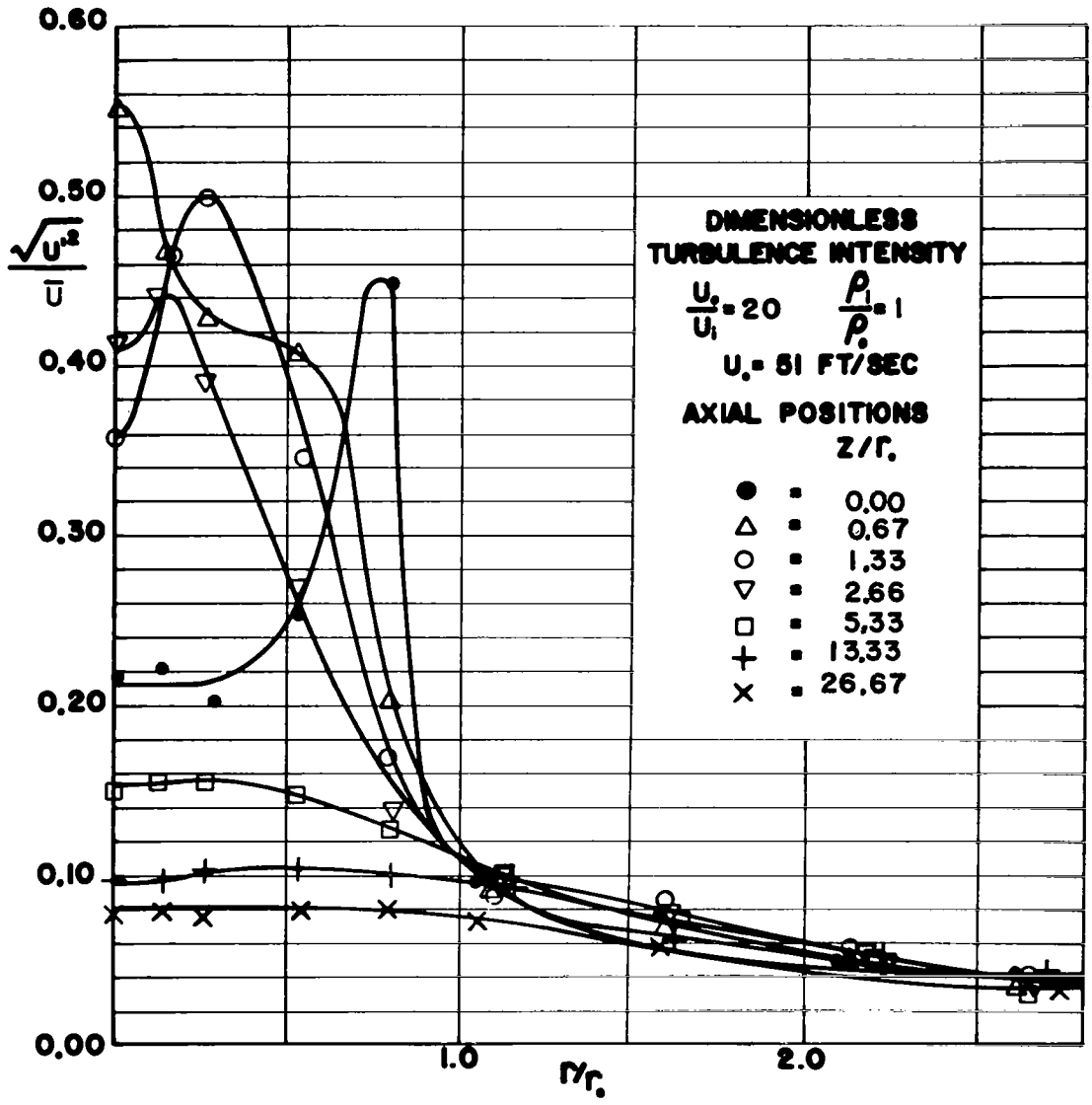

FIGURE 12

BOUNDARY LAYER TRIP DEVICE
AXIAL TURBULENCE INTENSITY PROFILES, HOMOGENEOUS

Heterogeneous Cases

Screen data for the 20 to 1 velocity ratio for the air Freon-12 system are presented in figures 13 through 18. The average velocity, density and turbulence intensities are shown.

There exists a region just downstream of the jet orifice where pure Freon-12 is found. This region is termed the potential core region and is conical in shape. The length of the potential core region varies inversely with the velocity ratio.

Figures 19 and 20 show the velocity and density profiles for a 12.25 to 1 velocity ratio with the boundary layer trip device.

Figures 17 and 18 show the velocity turbulence intensity profiles for the 20 to 1 velocity ratio. The heterogeneous profiles do not have a rate of increase of the centerline turbulence level nearly as great as do the homogeneous profiles. The homogeneous profiles tend to have the peak turbulence intensity close to the centerline, whereas the heterogeneous profiles have the peak further away from the centerline and this peak dies out before the centerline velocity turbulence intensity reaches a value equal to the original peak value.

When compared to the case of no boundary layer devices, the heterogeneous velocity turbulence intensity profiles show that not only is the overall turbulence level decreased, but that the peaking and spreading of the profiles are retarded to a position further downstream. This indicates that the mixing should be retarded by two effects, the lowering of the turbulence level and the buffer layer effects.

Figure 21 shows the mass holdup as a function of downstream position. The first 3 profiles were taken with the screen in place and an outer stream velocity of 51 ft/sec. The fourth profile, 12.25 to 1, was taken with the boundary layer trip device in place of the screen. This profile had the same inner jet mass flow rate as did the 20 to 1 screen case, but with a lower outer stream velocity. The last profile, 20.3 to 1, was taken from Zawacki's data which was taken in the same

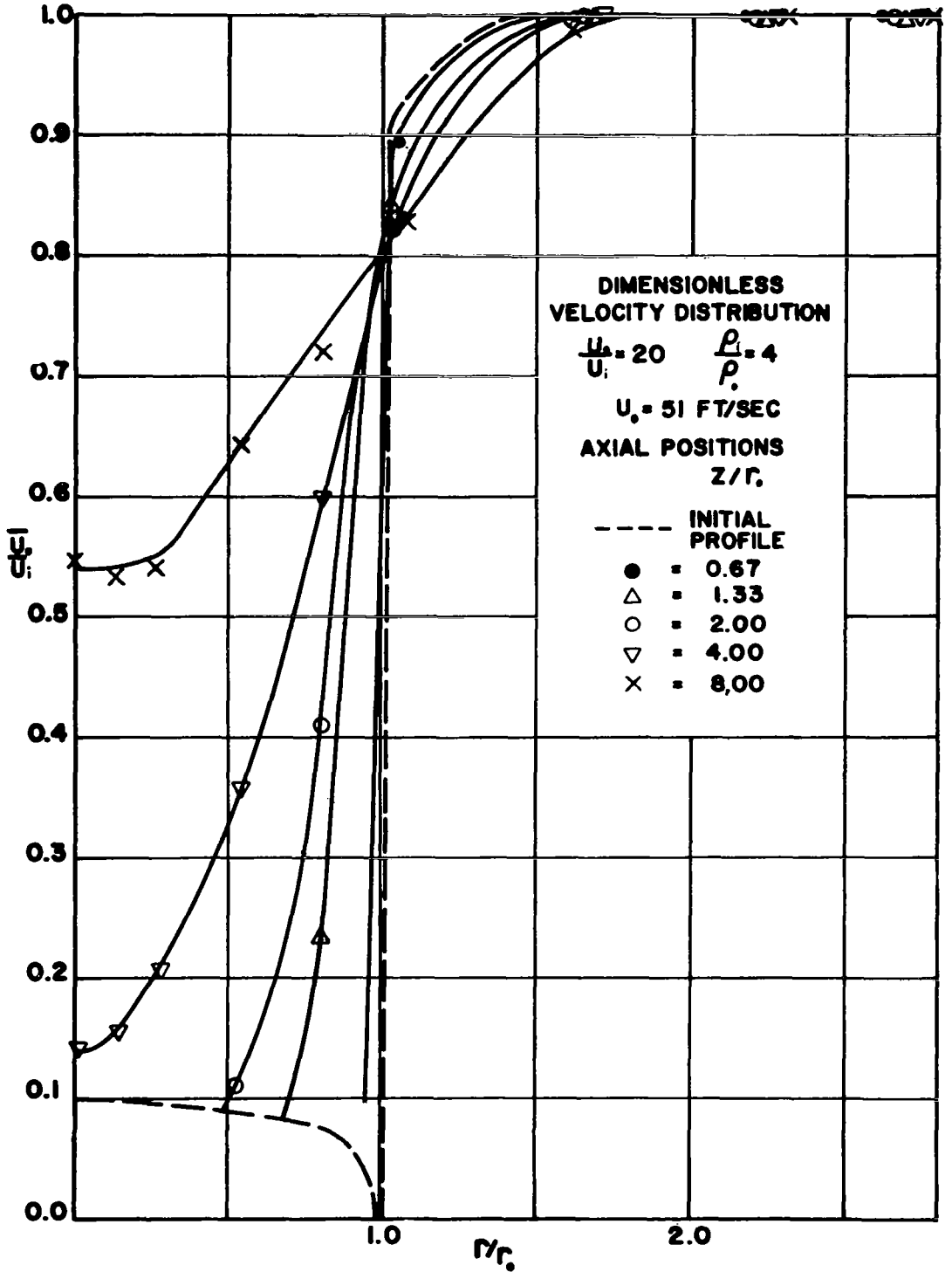

FIGURE 13

DIMENSIONLESS VELOCITY PROFILES, HETREOGENEOUS

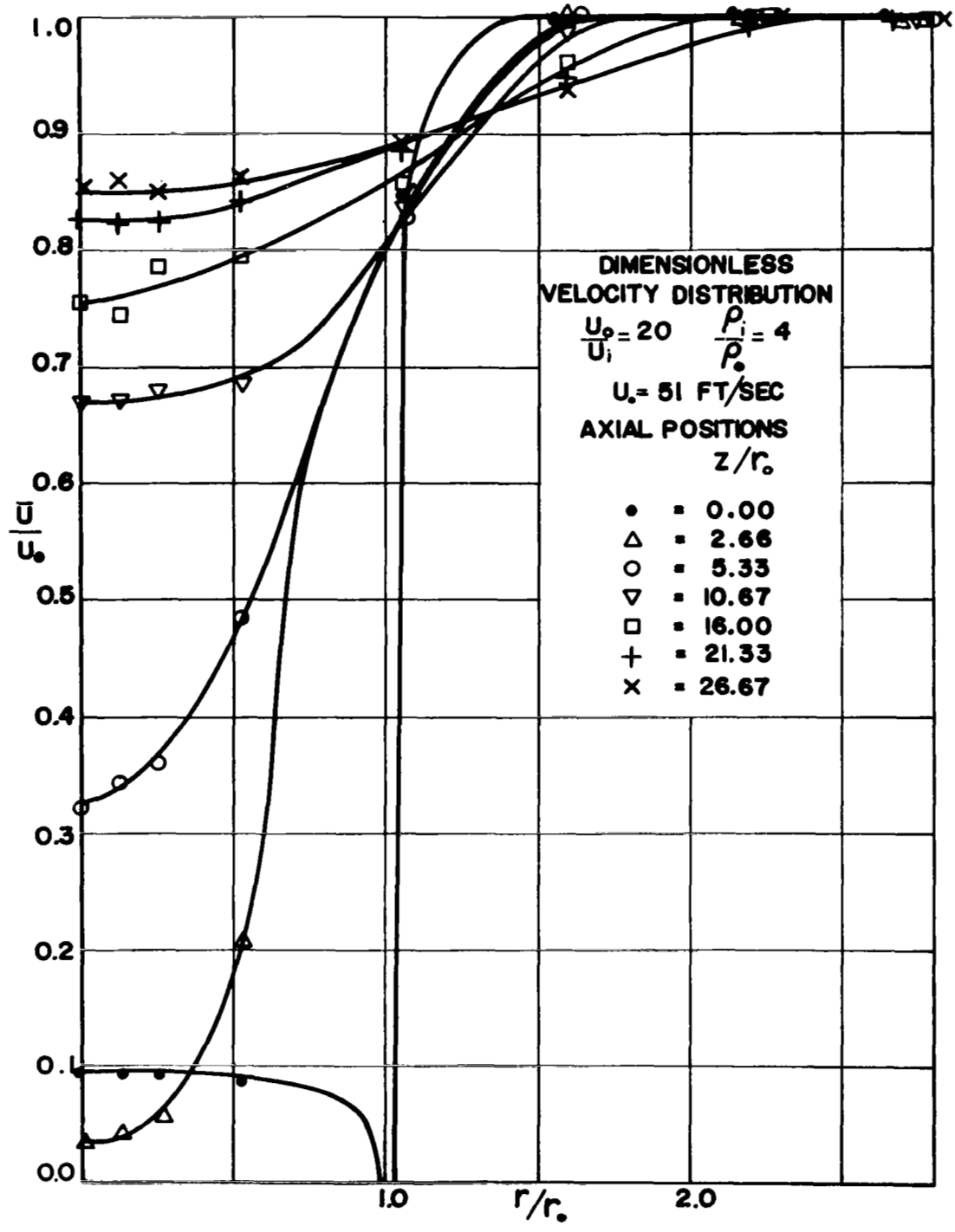

FIGURE 14

DIMENSIONLESS VELOCITY PROFILES, HETREOGENEOUS

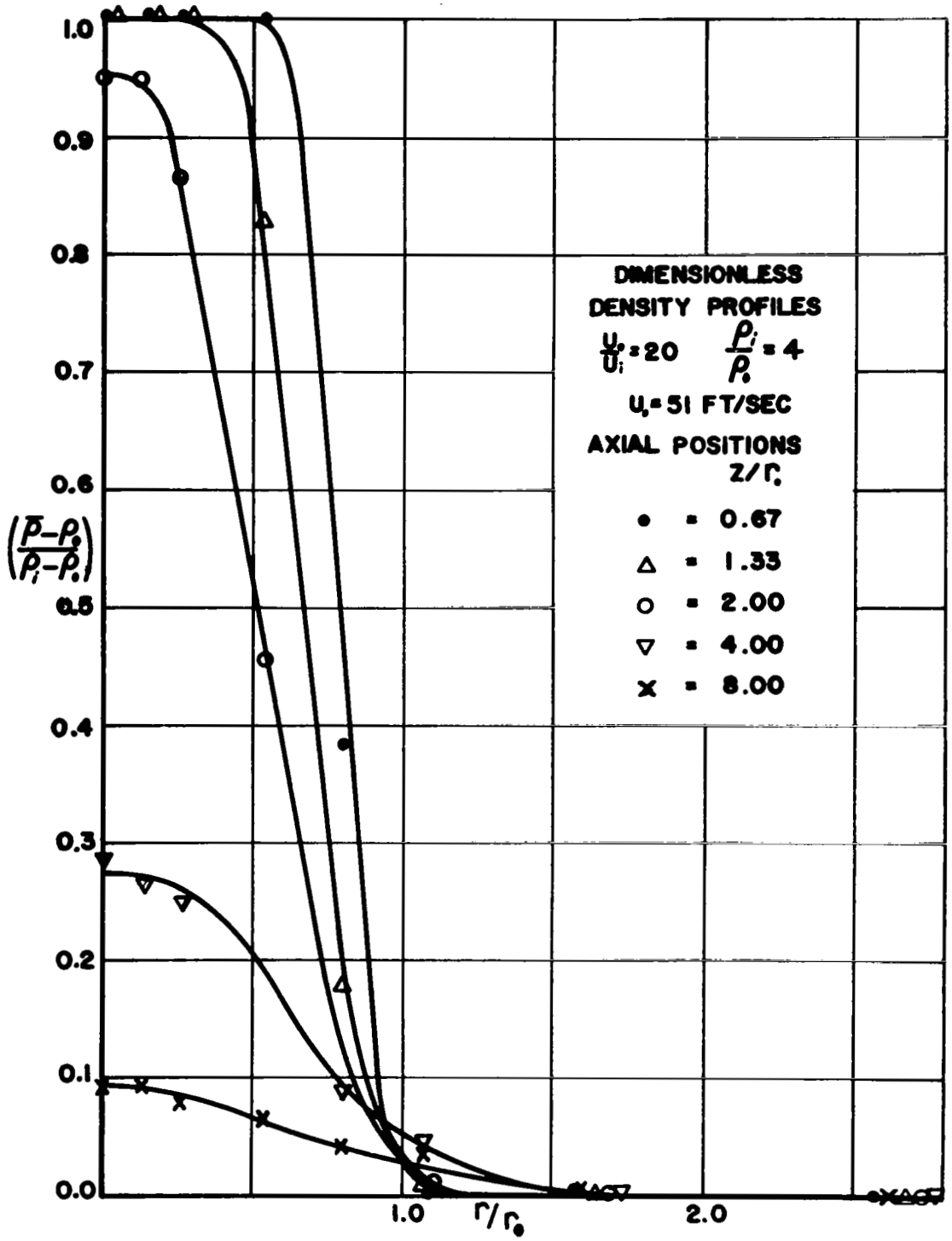

FIGURE 15

CONCENTRATION PROFILES

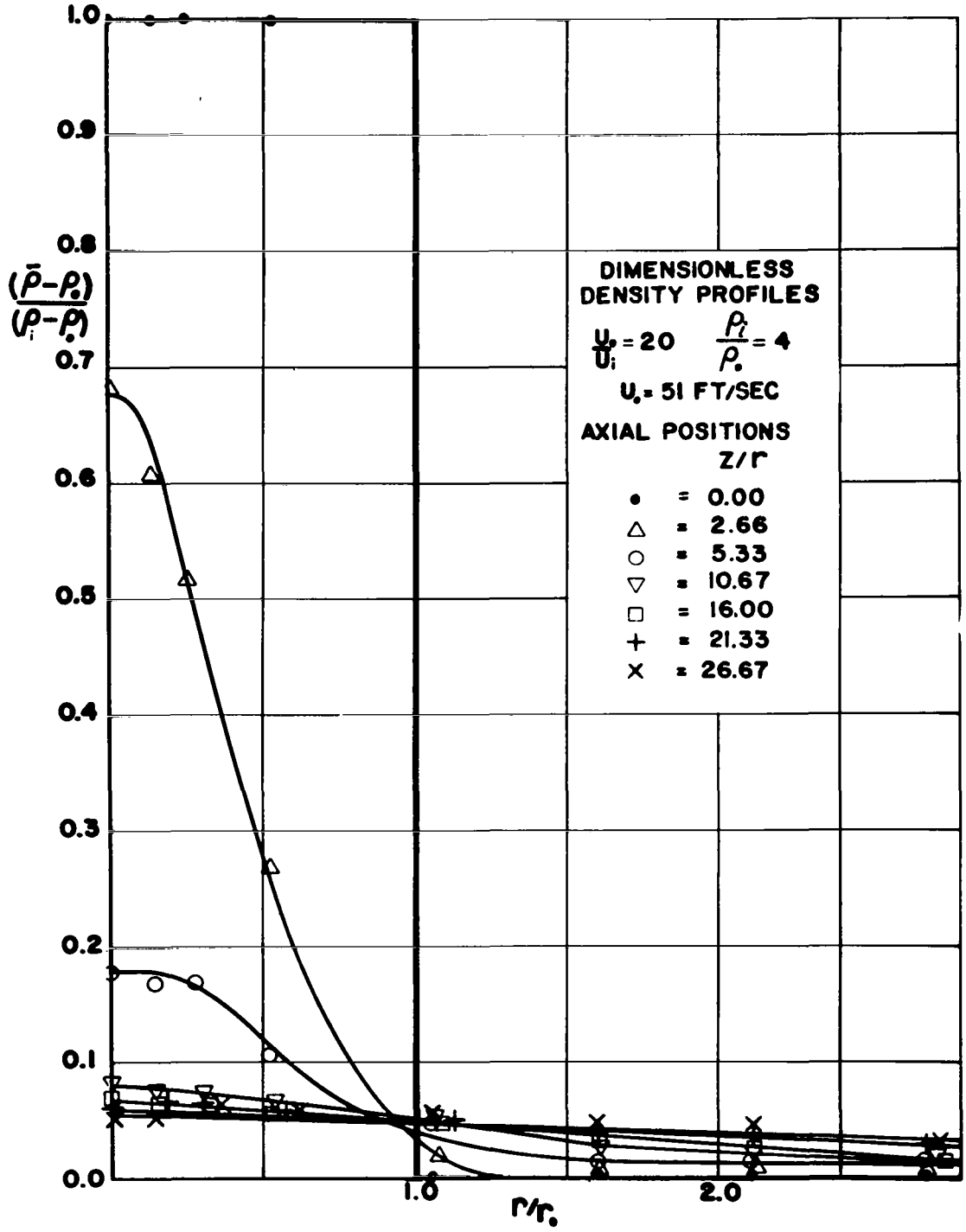

FIGURE 16

CONCENTRATION PROFILES

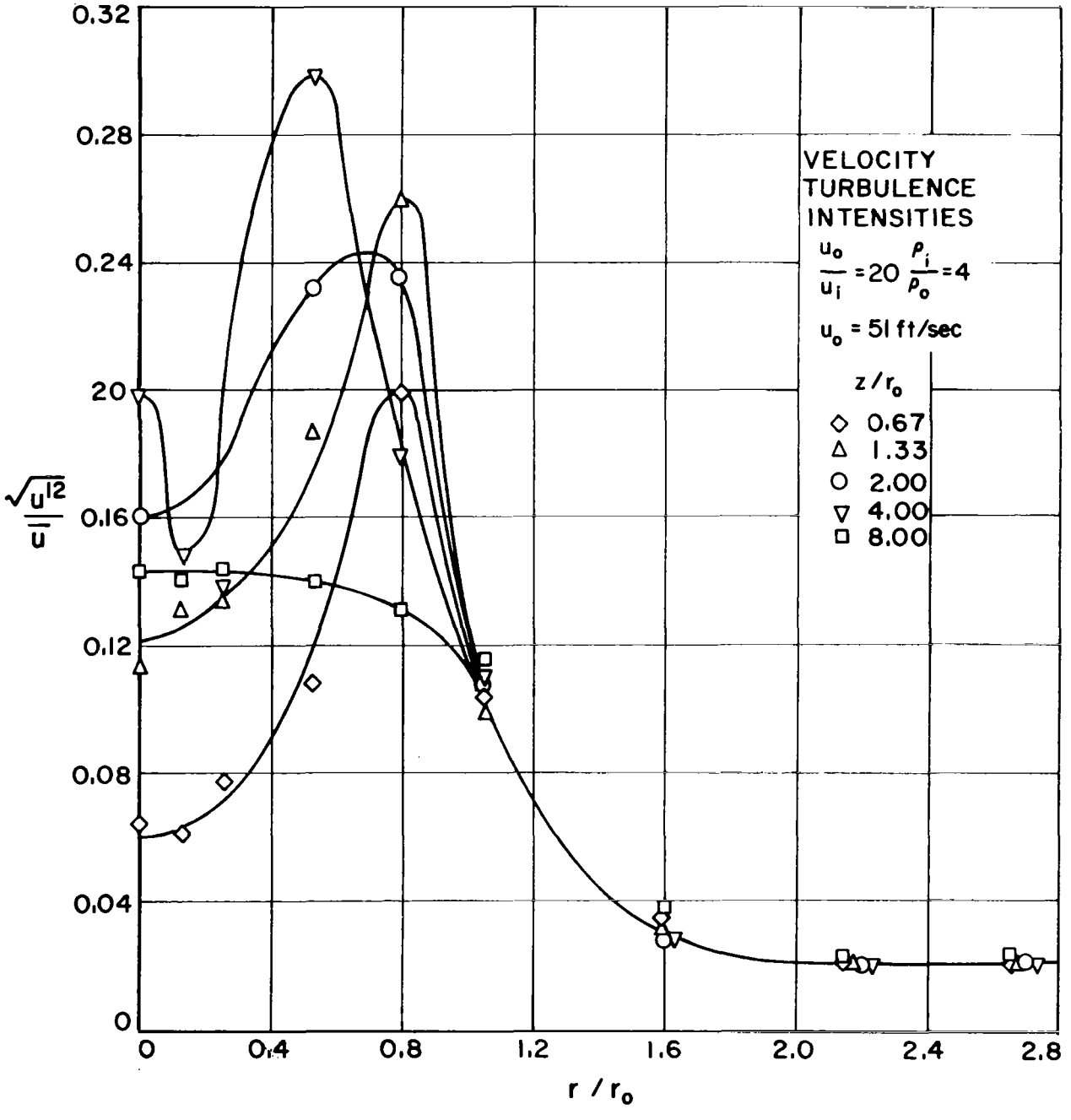

FIGURE 17

SCREEN DATA

VELOCITY TURBULENCE INTENSITY PROFILES, HETEROGENEOUS

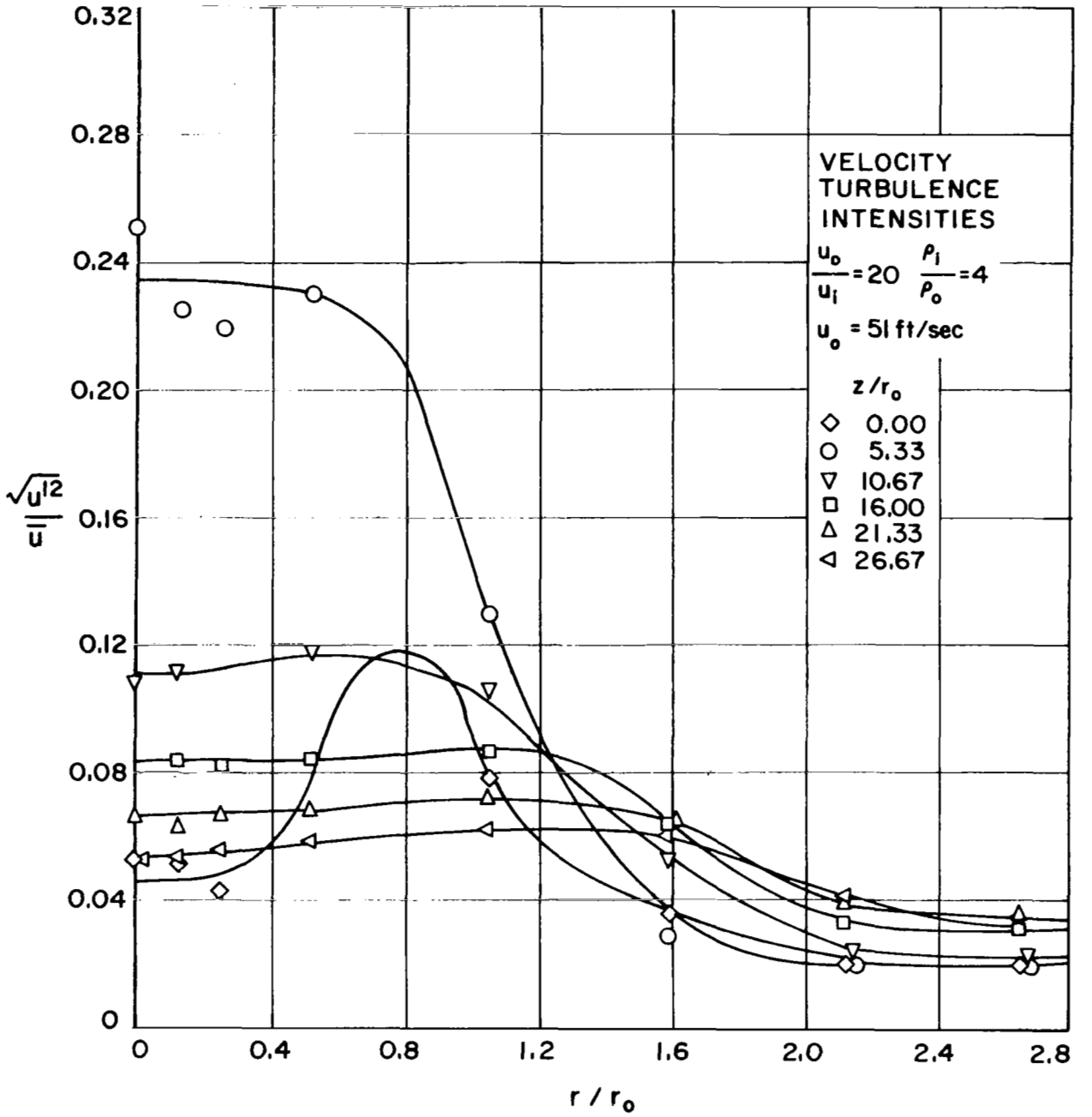

FIGURE 18

SCREEN DATA

VELOCITY TURBULENCE INTENSITY PROFILES, HETEROGENEOUS

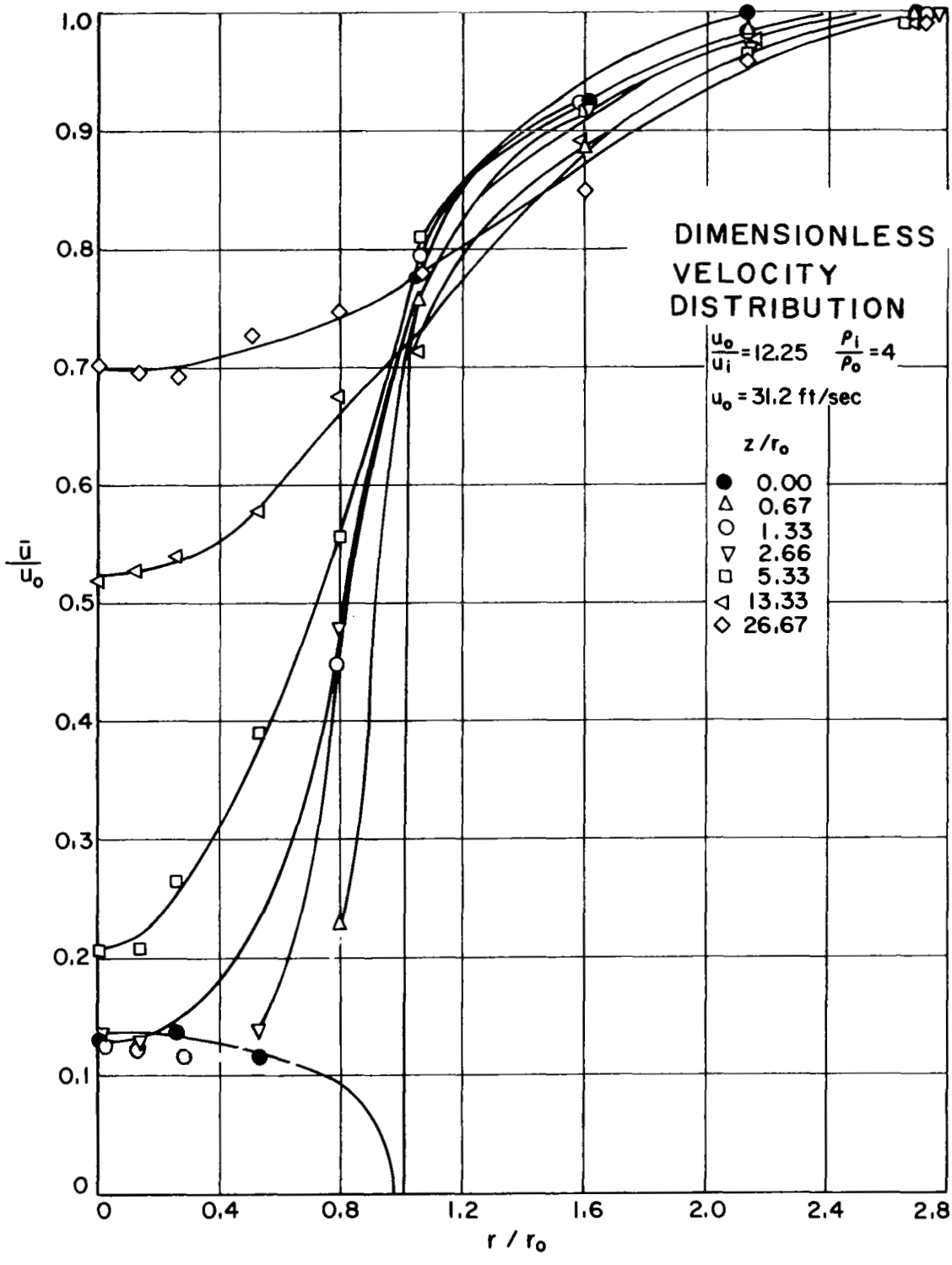

FIGURE 19

DIMENSIONLESS VELOCITY PROFILES, HETEROGENEOUS

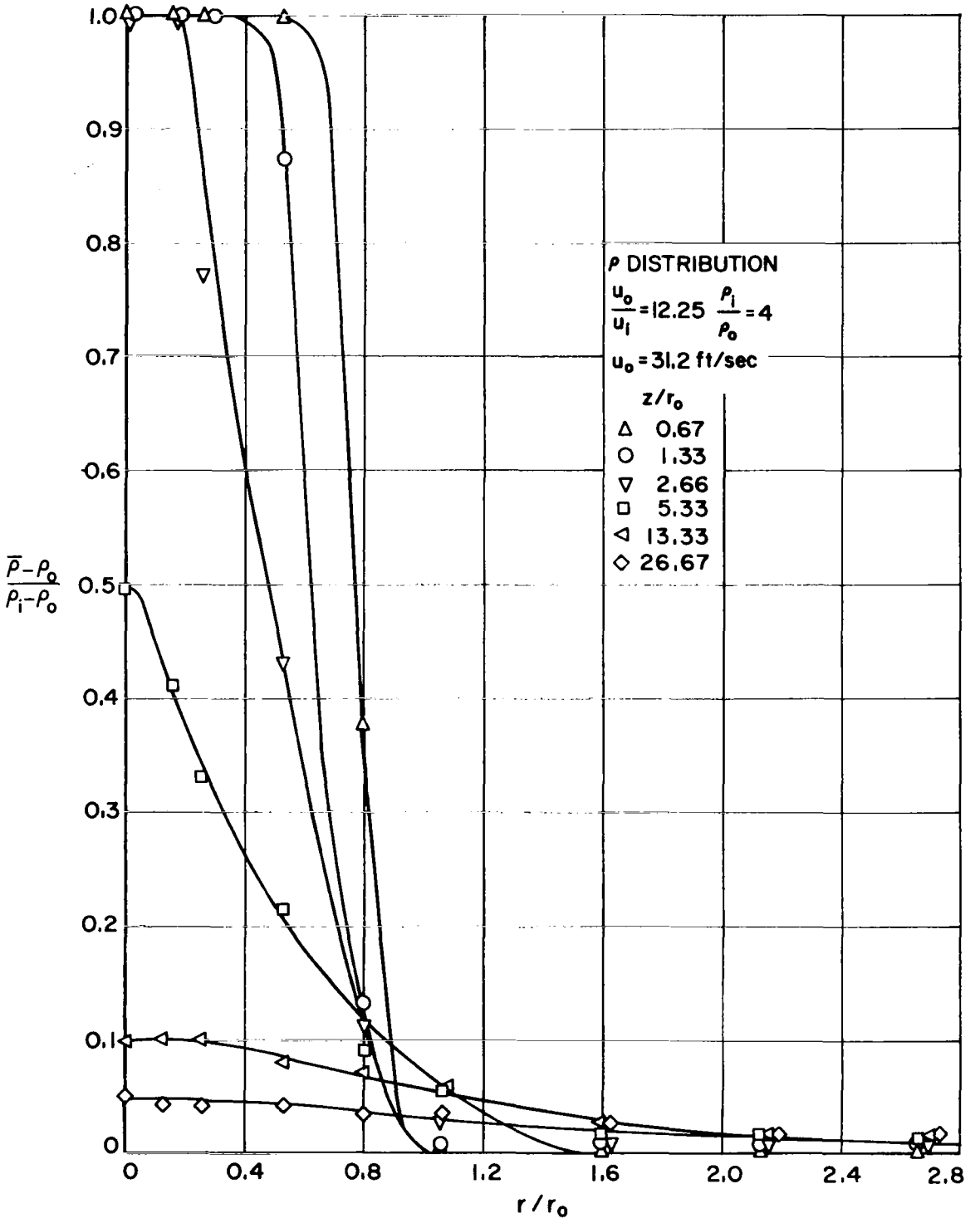

FIGURE 20

CONCENTRATION PROFILES

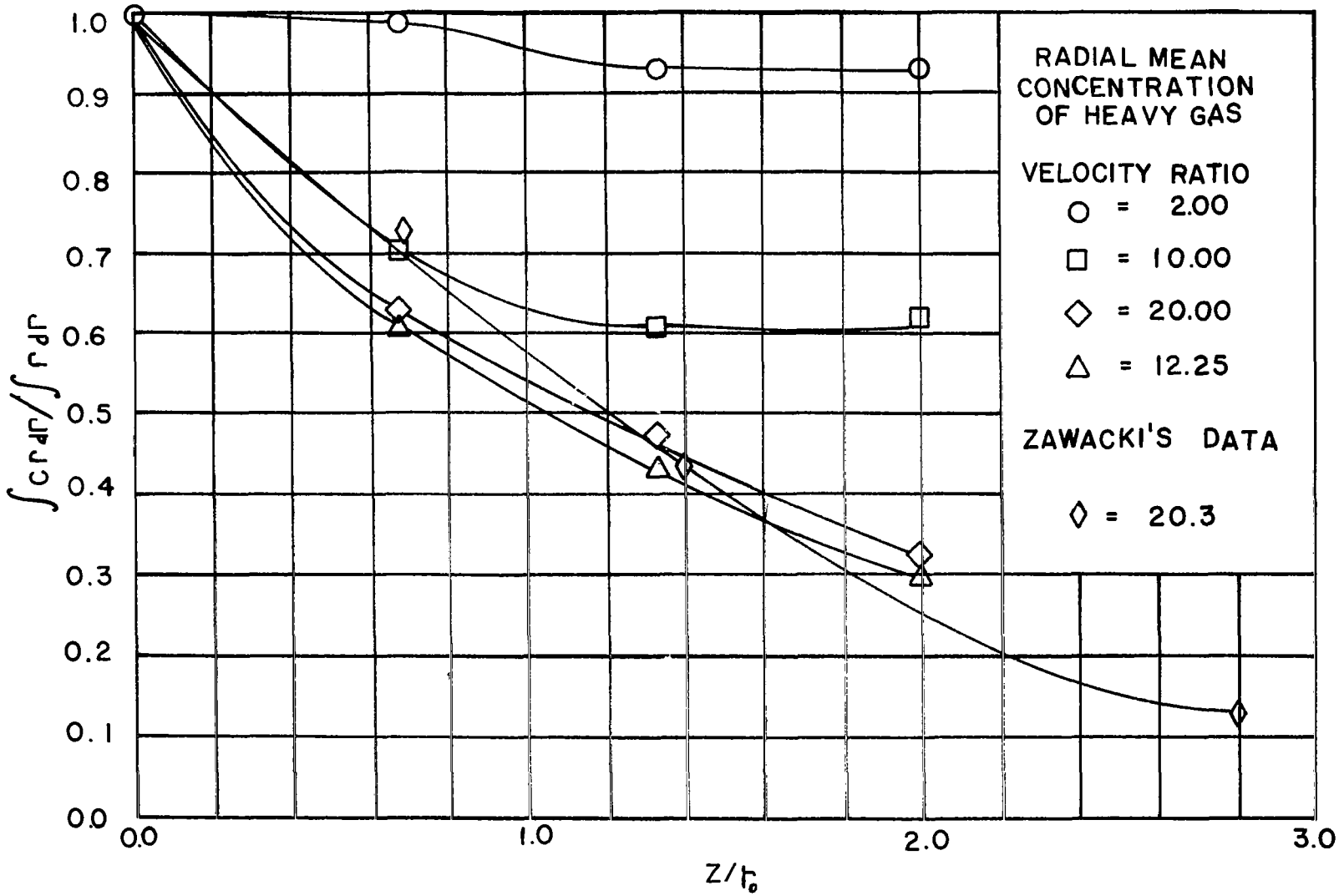

MASS HOLDUP FIGURE 21

equipment without either the screen or boundary layer trip device in place. It can be seen that for values of $Z/r_o > 2.0$, Zawacki's mass holdup continues to drop, whereas all the other runs with the screen or boundary layer trip device are leveling off.

The 2 to 1 velocity ratio exhibits the potential core effect to a position of $Z/r_o \approx 0.8$ then exhibits the same mixing effect as do the other profiles.

The boundary layer trip device data exhibits the same type of behavior as does the higher velocity ratio screen data. This could be caused by two factors. First, the screen causes a pressure drop in the outer stream whereas the boundary layer trip device does not. Thus the boundary layer on the outside of the inner tube is re-established more rapidly with the screen than with the boundary layer trip device, providing for a more effective buffer layer to retard the mixing. Second, the lower free stream turbulence intensity caused by the screen may retard mixing in the developing mixing region resulting in the larger mass holdup.

Zawacki's data exhibits greater inner stream preservation for small values of Z/r_o. This is probably due to the relatively large boundary layer on the outside of the inner tube which acted as a buffer region between the jets. As the boundary layer is accelerated, the jet behaves in much the same way as the other two cases but the point at which the "similar" region of the flow begins is later than in the other two cases.

Table 1 gives a comparison of the screen data with that of Zawacki.

Table 1

Z/r_o	$\left(\frac{\rho - \rho_o}{\rho_i - \rho_o}\right)_{\text{℄}}$	$\frac{u_o}{u_i}$	Z/r_o	$\left(\frac{\rho - \rho_o}{\rho_i - \rho_o}\right)_{\text{℄}}$	$\frac{u_o}{u_i}$
10	0.65	5	11.2	0.42	5.8
5.5	0.50	10	5.6	0.35	11.6
5.33	0.175	20	5.6	0.09	20.3

It can be seen for similar Z/r_o positions at almost equal velocity ratios the Freon-12 concentration is always considerably higher for the screen data than for the free jet data. In all cases however, at "sufficient" Z/r_o positions, the Freon is uniformly distributed over the entire jet since the outer jet is not, in fact, infinite. Thus all the mass holdup curves can be expected to asymptotically approach a final value given by the mass average injection rate divided by the area of the jet.

Table 2 compares the centerline density and density and velocity half-radii with velocity ratio for the screen data, the boundary layer trip device data, and Zawacki's data.

Table 2

Z/r_o	$\left(\frac{\rho - \rho_o}{\rho_i - \rho_o}\right)_{\mathcal{L}}$	$\frac{u_o}{u_i}$	$r_{1/2\,u}$	$r_{1/2\,\rho}$
		Screen Data		
5.5	0.50	10	0.85	0.45
13.33	0.125	10	1.20	1.20
5.33	0.225	15	0.75	0.75
13.33	0.090	15	1.05	1.10
5.33	0.175	20	0.75	0.70
10.67	0.075	20	1.10	1.20
		Boundary Layer Trip Device Data		
5.33	0.50	12.25	0.85	0.40
13.33	0.10	12.25	1.15	1.10
		Zawacki's Data		
5.33	0.09	20.3	0.80	0.90

Comparison of the density half radius of Zawacki's 20.3 to 1 data to that of the 20 to 1 screen data case indicates that the upstream screen decreases the spreading rate of the inner stream. Initial containment of inner stream fluid may be higher in Zawacki's case but once the increased spreading rate is felt by the inner stream, centerline density falls much faster than when the screen is present. It appears from this table that for both the screen and boundary layer trip device, the turbulent Schmidt number in the early mixing region ($Z/r_o = 5.33$) is different from that of Zawacki's data, since the velocity half radii are about the same both with and without the screen or boundary layer trip device while the density half radius is decreased by the presence of the screen or boundary layer trip device.

From the close agreement of average density and density and velocity half radii between the 10 to 1 screen case and the 12.25 to 1 boundary layer trip device case, it is evident that the average centerline density and the density and velocity half radii are dependent on the velocity ratio.

Since both the 12.25 to 1 boundary layer trip device case and the 20 to 1 screen case had the same mass injection rate, and since Figure 21 shows about the same mass holdup for both, the strong dependence of mass holdup on mass injection rate becomes evident.

CONCLUSIONS

Homogeneous System

1. As was found by Zawacki for large velocity ratios, wake flow predominates in the early mixing region even with either the screen or the boundary layer trip device.

2. For low velocity ratios there is less momentum transfer from the outer to the inner stream with the screen and the boundary layer trip device than without such devices.

3. For large velocity ratios there is no observable affect of either the screen or the boundary layer trip device.

4. The affect on mixing of the screen is mainly one of a boundary layer separation since there is no significant difference between the screen profiles and the boundary layer trip device profiles.

Heterogeneous System

1. Comparison of the data taken with the screen or the boundary layer trip device shows little difference. There is a significant difference however when either set of data are compared to the data of Zawacki taken without either type of device.

For low velocity ratios, the Freon-12 jet maintains its integrity much better with either the screen or the boundary layer trip device than without them. For high velocity ratios the wake affect predominates over the effect of either the screen or the boundary layer trip device.

2. The mass balance and the simple thread experiment indicate that standing circulation patterns do exist.

3. The velocity ratio appears to determine the average density and velocity profiles while the mass injection rate appears to strongly influence holdup for a given initial velocity profile.

BIBLIOGRAPHY

1 Boussinesq, J., Comptes Rendius Voe 113, 9 and 49 (1891)

2 Prandtl, L., "Bemerkung zur Theories der Freien Tubuelenz", ZAMM 22, 5 (1942).

3 Taylor, G. I., "The Transport of Vorticity and Heat Through Fluids in Turbulent Motion", Proc. Roy. Soc., (London), A135, 685, (1932).

4 Karman, Th. von: J. Aeronaut. Sce., Vol. 4, 131 (1937) .

5 Reichardt, H., "Gesetzmassigkeiten der Freinen Turbulenz", VDI- Forschungsh, 414 (1951) .

6 Kobashi, Y. and Tani, I., "Experimental Studies on Compound Jets", Proceedings of the Second Japan National Congress for Applied Mechanics, 465-468 (1951).

7 Kobashi, Y., "Experimental Studies on Compound Jets", Proceedings of the Second Japan National Congress for Applied Mechanics, 223-236 (1952).

8 Boehman, L., "Mass and Momentum Transport Properties in Isoenergetic Coaxial Flows", Ph.D. Thesis, Illinois Institute of Technology, (1967).

9 Alpinieri, L. J., "An Experimental Investigation of the Turbulent Mixing of Non-Homogeneous Coaxial Jets" Polytechnic Institute of Brooklyn, PIBAL Rept. 789, (1963): "Turbulent Mixing of Coaxial Jets", AIAA Journal, Vol. w, 1560-1568 (1964).

10 Zawacki, T. S. "Turbulence in the Mixing Region Between Coaxial Streams", Ph. D.Thesis, Illinois Institute of Technology, (1967).

11 D'Souza, G. J., "Turbulent Correlations in a Coaxial Flow of Dissimilar Fluids", M S. Thesis, Illinois Institute of Technology, (1967).

12 Montealegre, A. P., "Evaluation of Turbulence Correlations in a Coaxial Flow of Dissimilar Fluids", M. S. Thesis, Illinois Institute of Technology, (1967).

13 Forstall, W. Jr., and Shapiro, A. H., "Momentum and Mass Transfer in Coaxial Jets", Journal of Applied Mechanics, Vol. 17 No. 12, 399-408 (1950)

14 Frenkiel, F. N., "The Decay of Isotropic Turbulence", Journal of Applied Mechanics, Dec. 311-321 (1948).

15 Howard, C. D. and J. C. Laurence, "Measurement of Screen-Size Effects on Intensity, Scale, and Spectrum of Turbulence in a Free Subsonic Jet", NASA Technical Note D - 297.

16 Conger, W. L. "Measurement of Concentration Fluctuations in the Mixing of Two Gases by Hot Wire Anemometer Techniques", Ph.D. Thesis, Univ. of Pa. (1965).

17 Johnson, Bruce V., "Experimental Study of Multi-Component Coaxial-Flow Jets in Short Chambers", United Aircraft Research Laboratories Report 6910091-16, (April, 1968).

18 King, L. V., Phil. Trans. Roy. Soc. London, 214A, 373 (1914).

19 Kramer, H., Phsyca, 12, 61 (1946).

20 Leithem, J. "Turbulence Measurements in the Confined Coaxial Flow of Dissimilar Fluids", M. S. Thesis, Illinois Institute of Technology, (1968),

21 Kulik, R. A., "The Effect of Free Stream Turbulence on Coaxial Mixing", M. S. Thesis, Illinois Institute of Technology, (1968).

NASA-Langley, 1969 —— 12 E-4836